TMEM175 deficiency impairs lysosomal and mitochondrial function and increases α-synuclein aggregation

Sarah Jinn[a,b], Robert E. Drolet[c], Paige E. Cramer[c], Andus Hon-Kit Wong[a], Dawn M. Toolan[c], Cheryl A. Gretzula[c], Bhavya Voleti[c], Galya Vassileva[d], Jyoti Disa[a], Marija Tadin-Strapps[a], and David J. Stone[b,1]

[a]Target and Pathway Biology, Genetics and Pharmacogenomics, Merck Research Laboratories, Merck & Co., Inc., Boston, MA 02115; [b]Genetics, Genetics and Pharmacogenomics, Merck Research Laboratories, Merck & Co., Inc., West Point, PA 19486; [c]Neuroscience, Merck Research Laboratories, Merck & Co., Inc., West Point, PA 19486; and [d]Genomic Sciences, Genetics and Pharmacogenomics, Merck Research Laboratories, Merck & Co., Inc., Boston, MA 02115

Edited by Edward Scolnick, Massachusetts Institute of Technology, Cambridge, MA, and approved January 13, 2017 (received for review September 30, 2016)

Parkinson disease (PD) is a neurodegenerative disorder pathologically characterized by nigrostriatal dopamine neuron loss and the postmortem presence of Lewy bodies, depositions of insoluble α-synuclein, and other proteins that likely contribute to cellular toxicity and death during the disease. Genetic and biochemical studies have implicated impaired lysosomal and mitochondrial function in the pathogenesis of PD. Transmembrane protein 175 (TMEM175), the lysosomal K^+ channel, is centered under a major genome-wide association studies peak for PD, making it a potential candidate risk factor for the disease. To address the possibility that variation in TMEM175 could play a role in PD pathogenesis, TMEM175 function was investigated in a neuronal model system. Studies confirmed that TMEM175 deficiency results in unstable lysosomal pH, which led to decreased lysosomal catalytic activity, decreased glucocerebrosidase activity, impaired autophagosome clearance by the lysosome, and decreased mitochondrial respiration. Moreover, TMEM175 deficiency in rat primary neurons resulted in increased susceptibility to exogenous α-synuclein fibrils. Following α-synuclein fibril treatment, neurons deficient in TMEM175 were found to have increased phosphorylated and detergent-insoluble α-synuclein deposits. Taken together, data from these studies suggest that TMEM175 plays a direct and critical role in lysosomal and mitochondrial function and PD pathogenesis and highlight this ion channel as a potential therapeutic target for treating PD.

TMEM175 | lysosome | mitochondria | α-synuclein | Parkinson disease

Genome-wide association studies (GWAS) have identified a large number of loci that alter the risk of developing Parkinson disease (PD) (1). Given the nature of idiopathic PD as a complex, multifaceted disease, these non-Mendelian variants typically result in small increases or decreases in disease risk. However, the causal variants under the majority of GWAS peaks have not been definitively identified (2, 3). Characterizing the biological function of genes located in GWAS-implicated regions in the context of molecular and cellular development of PD may help to identify pathways that are critical in the etiology of the disease.

Several genes associated with PD (both Mendelian and GWAS) function in the lysosomal degradation pathway. Lysosomal degradation serves as a key final step to resolve protein aggregation in the process of macroautophagy and chaperone-mediated autophagy, and mutations that impair this process have been suggested to cause α-synuclein aggregation and downstream cellular toxicity. Mutations in the lysosomal hydrolase glucocerebrosidase (GBA) substantially increase the risk of PD (4, 5) and have been reported to compromise lysosomal degradation and increase α-synuclein aggregation (6). Mutations in lysosomal type 5 P-type ATPase (ATP13A2), a lysosomal ATPase, cause early-onset Parkinsonian syndrome (7) and have also been shown to cause lysosomal impairment. ATP13A2 mutations are linked to impaired acidification, decreased proteolytic processing, reduced degradation of lysosomal substrates, diminished lysosomal-mediated clearance of autophagosome, and neurotoxicity via the accumulation of α-synuclein (8, 9). Vacuolar protein sorting-associated protein 35 (VPS35) deficiency, also linked to familial PD (10), has been shown to perturb the maturation step of cathepsin D (CTSD) by increasing mannose-6-phosplate receptor turnover, resulting in accumulation of α-synuclein in the lysosomes (11). VPS35 gene deletion in dopamine neurons has also been reported to result in accumulation of α-synuclein and dopamine neuron loss (12, 13).

Mitophagy, the selective autophagy of mitochondria, also requires lysosomal degradation (14) and has also been implicated in the pathogenesis of PD. Phosphatase and tensin homolog deleted on chromosome 10-induced putative kinase 1 (PINK1), a mitochondrial ubiquitin kinase, and parkin, an E3 ubiquitin ligase, together initiate ubiquitin-mediated autophagosome formation around mitochondria (15–18). Mutations in genes encoding these proteins cause early-onset parkinsonian syndrome (19, 20). Mutations in F-box protein 7 that also cause early-onset autosomal recessive PD (21, 22) were recently shown to act on the parkin-mediated mitophagy by directly interacting with PINK1 and parkin (23). Although there are varying degrees of α-synuclein pathology in PINK1 or parkin-associated PD cases, reduced respiratory capacity and increased susceptibility to oxidative stress by the impairment of mitochondria quality control was demonstrated to lead to dopaminergic neuronal damage (24, 25). Additionally, overexpression of PINK1 or parkin can protect cells against toxicity associated with reduced proteasome function induced by synuclein aggregation (26, 27). Although it remains to be determined whether dysregulation of mitophagy also

Significance

Genetic studies have identified potential risk factors that have helped elucidate biological pathways involved in the development of Parkinson disease (PD). However, the majority of genome-wide association studies-implicated loci contain multiple genes requiring further investigation to establish the causality of any nominated gene to the pathology of associated disease. Here, we provide functional evidence that deficiency of the lysosomal K^+ channel transmembrane protein 175, discovered under the third most-significant PD genome-wide association study peak, is critical for pathogenesis of PD by impairing lysosomal and mitochondrial function.

Author contributions: S.J., R.E.D., P.E.C., M.T.-S., and D.J.S. designed research; S.J., A.H.-K.W., D.M.T., C.A.G., B.V., G.V., and J.D. performed research; S.J. analyzed data; and S.J., R.E.D., P.E.C., and D.J.S. wrote the paper.

Conflict of interest statement: All of the authors are employed by Merck & Co.

This article is a PNAS Direct Submission.

Freely available online through the PNAS open access option.

[1]To whom correspondence should be addressed. Email: david_stone4@merck.com.

This article contains supporting information online at www.pnas.org/lookup/suppl/doi:10.1073/pnas.1616332114/-/DCSupplemental.

Downloaded at Palestinian Territory, occupied on December 16, 2021

NEUROSCIENCE

www.manaraa.com

contributes to sporadic PD, maintenance of mitochondrial health is clearly linked to the molecular pathology of PD.

Human transmembrane protein 175 (TMEM175), recently identified from a lysosomal proteome (28), is a K^+ channel located in late endosomes and lysosomes (29). A PD GWAS meta-analysis (1) identified a highly significant risk loci on chromosome 4, which covers several genes, including TMEM175. Identification of the candidate gene residing in this peak could be critical, not only to understanding the pathogenesis of PD but also in identifying a novel genetically validated therapeutic target for treating the disease. If in fact TMEM175 is the candidate gene, then as a K^+ channel there is a high potential for druggability and there is a tractable therapeutic strategy. TMEM175 appears a likely candidate, as it has been shown to regulate lysosomal membrane potential, pH stability, and organelle fusion via potassium conductance on lysosomal and endosomal membranes (29). To help resolve a potential link between TMEM175 and PD, we have characterized the effects of TMEM175 in the context of lysosomal and mitochondrial function, as well as the susceptibility to α-synuclein aggregation in both neuroblastoma and primary neuron cellular systems. We show that TMEM175 deficiency impairs lysosomal degradation, lysosome-mediated autophagosome clearance, and mitochondrial respiratory capacity. These cellular defects result in increased neuronal susceptibility to exogenously applied α-synuclein fibrils, a well-studied model of α-synuclein uptake, processing, and degradation. Our findings suggest that TMEM175 loss-of-function mutations likely impair autophagy-mediated degradation of α-synuclein oligomeric species and, moreover, that variation in TMEM175 may be in part responsible for the linkage of the chromosome 4:951,947 GWAS peak to PD risk.

Results

TMEM175 Deficiency Decreased Lysosomal Catalytic Activity in Neuronal Cells via Destabilized Lysosomal pH. TMEM175 was identified as a K^+ channel that mediates potassium conductance on lysosomal and endosomal membranes, and thus regulates lysosomal membrane potential and pH in RAW 246.7 murine macrophages (29). To determine if TMEM175 serves a similar function in cells of neuronal origin, knockout of TMEM175 (KO) was engineered in the SH-SY5Y neuroblastoma cell line using a CRISPR/Cas9 approach (Fig. 1*A*). Under fed conditions, in media containing 10% (vol/vol) serum, lysosomal pH of TMEM175 KO SH-SY5Y was slightly more acidic than WT. Upon starvation in Earle's Balanced Salt Solution (EBSS) for 3 h, a significant increase in lysosomal pH was observed, whereas WT SH-SY5Y cells maintained lysosomal pH in both fed and starved conditions (Fig. 1*B*). This result agrees with previous findings in TMEM 175 KO macrophage, and is expected given universal expression of TMEM175 in lysosomes throughout multiple tissues. Protein levels of lysosomal aspartyl protease, CTSD, and cysteine protease, cathepsin B (CTSB), were significantly decreased in TMEM175 KO cells relative to WT both in fed and starved conditions (Fig. 1*D*), suggesting lysosomal dysfunction. Faster migration of lysosome-associated membrane glycoprotein 1 (LAMP1) was also observed in TMEM175 KO cells relative to WT potentially by deglycosylation or proteolytic cleavage that could lead to their instability (Fig. 1*D,* second row) (30, 31). TMEM175 KO did not change the number of $LAMP1^+$ lysosomes (Fig. 1*C*). Further evaluation of the activities of these lysosomal enzymes revealed that CTSD, CTSB, and GBA, another lysosomal hydrolase linked to PD, were significantly decreased by 20–30% in TMEM175 KO compared with WT, as indicated by the smaller rate constant (k) (Fig. 1 *E*–*G*). Starvation did not further amplify the degree of enzyme activity reduction between WT and KO. This finding would suggest that additional mechanisms (beyond impaired pH regulation) may play a role in the reduced enzyme activity resulting from TMEM175 KO. Consistent with decreased activities of proteases, the rate of L-Homopropargylglycine (HPG)-labeled protein degradation was decreased in KO relative to WT (Fig. 1*H*).

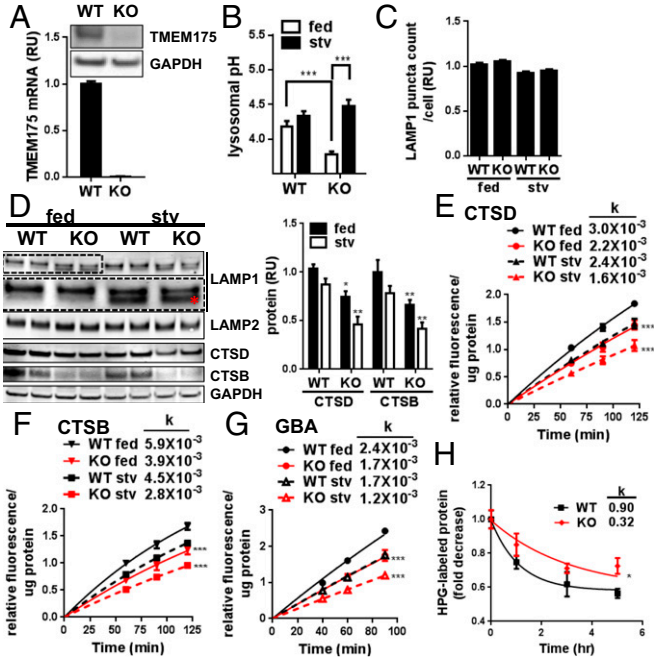

Fig. 1. Unstable lysosomal pH and reduced lysosomal enzyme activity in TMEM175 KO cells (*A*) Western blotting and quantitative real-time PCR (qRT-PCR) showing levels of TMEM175 in SH-SY5Y WT and TMEM175 KO cells. (*B*) Lysosomal pH of WT and KO was measured in fed (white) and starved (stv, black, EBSS 3 h) conditions (n = 6). (*C*) Number of $LAMP1^+$ lysosomes determined by immunohistochemistry and shown relative to WT (n = 5–7). (*D*) Protein levels of lysosomal CTSD and CTSB were quantified by Western blotting (*Left*) and shown normalized to glyceraldehyde 3-phosphate dehydrogenase (GAPDH) (*Right*, faster migrating LAMP1 in the second row is indicated with red asterisk) (n = 4). (*E*–*G*) Lysosomal enzyme activity of CTSD, CTSB, and GBA was determined by the relative fluorescence from enzyme activities of crude lysosomal fractions of WT and KO cells in fed (black) and starved (red) conditions (n = 3–4). Relative fluorescence as a function of time was fit to first order reaction with rate constants, k, for each group indicated on the right. (*H*) Relative intensity of HPG-labeled proteins after incorporation of HPG was plotted as a function of time and fit to one phase exponential decay (n = 3–5). The rate constant k is indicated on the right. Data are given in relative units (RU). Data presented are mean + SEM. Two-way ANOVA in *B*, *D*, *E*–*H*; Bonferroni's test in *C*, $^*P < 0.05$, $^{**}P < 0.01$, and $^{***}P < 0.001$ WT vs. KO.

We confirmed these results in primary rat hippocampal neuronal cultures. Transient knockdown (KD) of TMEM175 in primary neurons by siRNA (Fig. S1*A*) led to unstable pH compared with control siRNA, consistent with the above result in SH-SY5Y (Fig. S1*B*). TMEM175 knockdown did not affect the number of $LAMP1^+$ lysosomal counts (Fig. S1*C*). Depletion of TMEM175 also significantly decreased enzyme activity of CTSD, CTSB, and GBA by 20–35% relative to controls (Fig. S1 *E*–*G*), even though only CTSB protein level was decreased in TMEM175-depleted rat hippocampal neurons (Fig. S1*D*). This result could be because of a transient knockdown in this model instead of complete KO of TMEM175 in SH-SY5Y. The degradation rate of HPG-labeled proteins was also lower in TMEM175-depleted cells compared with controls (Fig. S1*H*). Taken together these results indicate that TMEM175 plays critical role in maintaining lysosomal pH and proper lysosomal enzyme function in neuronal cells.

TMEM175 Deficiency Impairs Clearance of Autophagosome After Accelerated Autophagosome–Lysosome Fusion. One major function of lysosomes as cellular catalytic machinery is to degrade

Downloaded at Palestinian Territory, occupied on December 16, 2021
www.manaraa.com

autophagy cargos through fusion with autophagosomes at the final step of autophagy. Digestion of engulfed materials is important for recycling amino acids and preventing the accumulation of aggregated proteins and aged organelles (14, 32). To determine if TMEM175 deficiency affects the process of autophagy, we evaluated the fusion of autophagosome to lysosome. To monitor the autophagosome, a RFP–GFP–LC3 construct was transiently transfected into TMEM175 KO SH-SY5Y cells. The signal of autophagosome-associated LC3 under fed conditions was evaluated. In this assay, pH-sensitive GFP signal (Fig. 2, green) is quenched by the acidic environment of lysosomes, although RFP signal (Fig. 2, red) is pH-insensitive. Thus, autophagosomes (AP, not fused to lysosomes) are marked by both GFP and RFP, whereas autophagolysosome (APL, fused to lysosomes) are marked only by RFP (Fig. 2*A*). The number of GFP puncta was significantly decreased in TMEM175 KO cells relative to WT cells, whereas the number of the total puncta mildly decreased, resulting in an overall decreased GFP (AP) and increased RFP-only (APL) puncta relative to total puncta (Fig. 2 *B* and *C*). This result suggests that a larger portion of autophagosomes are fused to lysosomes in TMEM175 KO cells, consistent with the previous finding that deficiency of TMEM175 leads to accelerated fusion of autophagosomes to lysosomes in RAW246.7 macrophage (29). To further determine whether TMEM175 deficiency affects the completion of autophagy, clearance of autophagy substrates was assessed. The endogenous level of microtubule-associated protein 1A/1B-light chain 3-II (LC3-II), which increases upon initiation of autophagy and is degraded as a part of autophagic cargo, was evaluated at multiple time points by Western blotting or immunocytochemistry in the absence and the presence of bafilomycin A. Without bafilomycin, autophagosome LC3 formation upon starvation (LC3-II/I ratio or LC3 puncta) peaked at 1 h and decreased afterward in WT, whereas there was a delayed degradation of LC3 in TMEM175 KO cells (Fig. 2 *D* and *E* and Fig. S2*A*), resulting in a significant increase in LC3 levels in TMEM175 KO cells relative to control at 3 and 5 h after starvation (Fig. 2 *F* and *G*, *Upper*). Adding bafilomycin resulted in accumulation of LC3 over time after the initiation of starvation to the same degree in both WT and TMEM175 KO cells, eliminating the difference in LC3 levels between WT and TMEM175 KO cells (Fig. 2 *D* and *E* and Fig. S2*A*) (+BafA1). This result indicates that reduction of LC3 in WT was indeed because of lysosomal degradation, and that inefficient lysosomal clearance of autophagosome but not autophagosome biogenesis was the cause of increased LC3 levels in TMEM175-deficient cells. Similarly, in rat primary hippocampal neurons, the autophagy substrate sequestosome1 (p62), as well as LC3 levels, were increased in TMEM175-depleted cells relative to control hippocampal neurons in both fed and starved conditions by immunocytochemistry (Fig. 2 *F* and *G*, *Lower*). Protein levels determined by Western blotting confirmed these findings (Fig. S2*B*), suggesting accumulation of autophagosomes. Given that the number of total autophagosomes is mildly decreased in TMEM175-depleted cells, increase levels of autophagosome substrates suggests that completion of autophagy is stalled because of impaired lysosomal degradation.

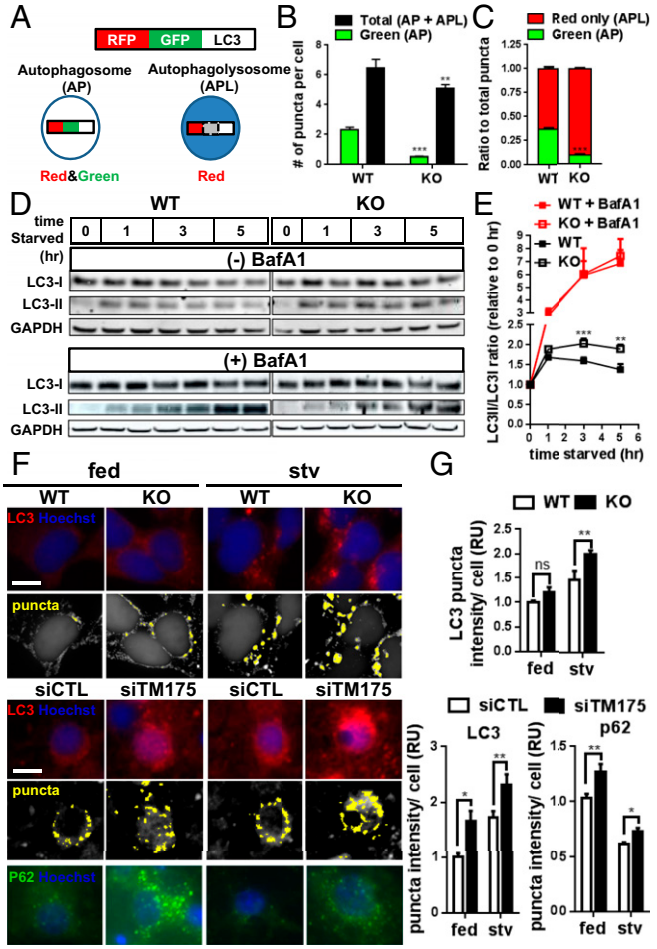

Fig. 2. TMEM175 deficiency leads to accelerated autophagosome–lysosome fusion and impairs clearance of autophagosome. (*A*) Schematic describing autophagosome–lysosome fusion assay with the RFP- and GFP-tagged LC3 construct transfected into WT and TMEM175 KO cells. (*B*) The number of green and total LC3 puncta from WT and KO cells was quantified ($n = 5$). (*C*) Ratio of GFP puncta or RFP only puncta to total is quantified ($n = 5$). (*D* and *E*) Level of autophagy substrate LC3 was measured at indicated time points by Western blotting in WT and KO cells with or without bafilomycin A1 (100 nM). Quantified ratio of LC3-II to LC3-I relative to time = 0 is shown ($n = 4$). Extra space between LC3-I and LC3-II was cropped to improve the clarity of images. (*F* and *G*) Autophagosome-associated LC3 puncta [red, *Top*, 5-h starvation, SH-SY5Y; *Middle*, 4-h starvation, rat hippocampal neurons treated with control (siCTL) or TMEM175 targeting (siTM175) shRNA], and p62 puncta (green, *Bottom*, rat hippocampal neurons) in fed and starved conditions were assessed by immunohistochemistry. Black and white contrast images of LC3 were highlighted with puncta quantified (yellow) (*F*). Quantified intensity of each puncta is plotted ($n = 5$) (*G*). (Scale bars, 10 μm.) Data presented are mean + SEM. Two-way ANOVA in *B, E, G*; Mann–Whitney test in *C*, $^{*}P < 0.05$, $^{**}P < 0.01$, and $^{***}P < 0.001$. WT vs. KO or siCTL vs. siTM175.

TMEM175 Deficiency Decreases Mitochondrial Respiration. Autophagy regulates mitochondrial turnover through multiple mechanisms of mitophagy, which establish energetic homeostasis and prevent mitochondrial aging in response to environmental cues (14, 33). Inhibition of autophagy can lead to decreased mitochondrial respiration through accumulation of dysfunctional mitochondria and deficits in metabolic substrates (34, 35). To determine whether decreased clearance of autophagosomes in TMEM175-deficient cells also affects mitochondrial energetic capacity, we measured mitochondrial oxygen consumption rate (OCR). There were significant decreases in basal as well as maximal mitochondrial OCR in TMEM175 KO SH-SY5Y cells relative to WT cells (Fig. 3 *A* and *B*). Maximal OCR was determined from the difference between carbonyl cyanide-p-trifluoromethoxyphenylhydrazone (FCCP)-induced OCR and Oligomycin A-induced OCR. Oligomycin A inhibited complex V of the electron transport chain to decrease oxygen consumption to a similar degree between TMEM175 KO and WT cells. Therefore, maximal OCR was reduced primarily because of a decrease in uncoupled respiration induced by a range of FCCP concentrations (Fig. S3 *A* and *B*), which cause maximal electron transfer through the electron transport chain independent of ATP synthesis. This finding indicates considerably compromised

Downloaded at Palestinian Territory, occupied on December 16, 2021
www.manaraa.com

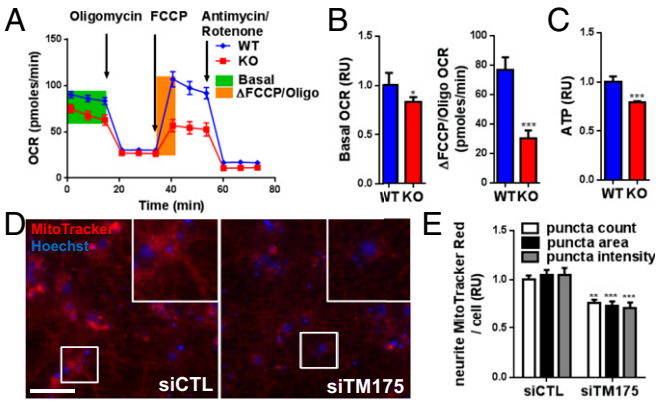

Fig. 3. Mitochondrial respiration is decreased by TMEM175 depletion. (*A*) OCR of SH-SY5Y WT and TMEM175 KO cells were measured in real time. (*B*) Basal OCR and the difference between FCCP-induced OCR and Oligomycin A-induced OCR were plotted ($n = 9$–11). (*C*) Total intracellular ATP normalized to protein was plotted ($n = 9$). (*D* and *E*) Representative images of MitoTracker Red staining of siCTL and siTM175-treated rat hippocampal neurons were shown (*D*). (Scale bar, 50 μm.) Quantification of intensity, area and number of MitoTracker Red puncta in neurites was plotted (*E*) ($n = 6$). Data presented are mean + SEM. Mann–Whitney test in *B* and *C*; two-way ANOVA in *E*, $*P < 0.05$, $**P < 0.01$, and $***P < 0.001$. WT vs. KO or siCTL vs. siTM175.

respiratory capacity in TMEM175-deficient cells compared with WT cells. Transient depletion of TMEM175 (siTM175) in rat hippocampal neurons also led to decrease in maximal OCR (Fig. S3 *C* and *D*), although to a lesser degree than complete KO. Consistent with this result, total ATP levels were decreased in TMEM175-depleted cells relative to controls because of a decrease in mitochondrial oxidative phosphorylation (Fig. 3*C* and Fig. S3*E*). In primary neurons, this decrease also coincides with reductions of MitoTracker staining, which accumulates in active mitochondria, particularly in neurites, suggesting diminished migratory ability of active mitochondria (Fig. 3 *D* and *E*). Because TMEM175 is localized to lysosomes and endosomes, and does not appear to be expressed in mitochondria as shown by MitoFates (36) and MitoCarta (37) prediction of mitochondrial localization, decreased respiration is likely mediated by lysosomal impairment. Together, these findings suggest that reduction of TMEM175 expression leads to deficits in energy homeostasis through impaired lysosome-mediated mitophagy.

TMEM175 Deficiency Increases Phosphorylated α-Synuclein Aggregates in Rat Primary Hippocampal Neurons. Impaired completion of autophagy in TMEM175-deficient cells strongly suggests that TMEM175 might influence α-synuclein aggregation, the clearance of which is often mediated by autophagy. To determine if TMEM175 plays a role in α-synuclein aggregation, we used a previously published method of seeding preformed α-synuclein fibrils (PFF) (38, 39) in rat hippocampal neuronal cultures. In this model, exogenously provided human α-synuclein PFF recruits endogenously expressed rat α-synuclein, which is essential to form aggregates that are characterized by hyperphosphorylation and detergent insolubility. Rat hippocampal neurons were seeded with human α-synuclein PFF after preinfection with lentiviral control shRNA (shCTL) or TMEM175 shRNA (shTM175) and incubated for an additional 14 and 21 d, after which they were evaluated for the phosphorylated α-synuclein by immunocytochemistry and Western blotting (Fig. 4*A*). shRNA against TMEM175, which resulted in ∼75–80% KD of TMEM175 relative to control shRNA in 14- and 21-d cultures (Fig. 4*B*). In PFF-treated TMEM175-KD neurons, a significant ∼2- to 3-fold (14 d) (Fig. 4 *C* and *D*) and ∼1.5 fold (21 d) (Fig. 4 *G* and *H*) increase in phosphorylated α-synuclein staining was observed compared with control PFF-treated neurons. This increase was independent of types of shRNAs used and correlated with the degree of TMEM175 depletion (Fig. S4*A*). Depletion of TMEM175 alone did not change the endogenous levels of α-synuclein in PBS-treated groups (Fig. S4*B*). There was no change in cell viability assessed by the number of healthy nuclei or metabolic activity in TMEM175-KD neurons at 14 d after PFF (Fig. 4*E*). Viable cells decreased at 21 d after PFF (Fig. 4*I*), potentially contributing to attenuated fold-increase in phosphorylated α-synuclein compared with 14 d after PFF. Importantly, the pathologically relevant, phosphorylated oligomers of α-synuclein in the detergent-insoluble fraction were also increased by ∼1.7-fold (14 d) (Fig. 4*F*, *Upper*) and ∼1.4-fold (21 d) (Fig. 4*J*, *Upper*) in TMEM175-deficient neurons relative to control neurons. Phosphorylated α-synuclein monomers in the Triton X-100 soluble fraction were also increased in TMEM175-deficient neurons relative to control neurons (Fig. S4*C*). Total α-synuclein levels detected by antibody that recognizes both human and rat α-synuclein remained unchanged in both detergent-insoluble and insoluble fractions (Fig. 4 *F* and *J*, *Lower*, and Fig. S4*C*). Taken together, these results suggest that TMEM175 appears to play a critical role in α-synuclein dynamics and depletion of TMEM175 leads to increased propensity for accumulation of α-synuclein aggregates, which is the key factor in α-synucleinopathies and the development of PD.

Discussion

Genetic studies have identified potential risk factors that have helped elucidate biological pathways involved in the development PD. However, the majority of GWAS-implicated loci contain multiple genes requiring further work, such as sequencing, integrative approaches such as Mendelian randomization, and wet-laboratory biological validation to establish the causality of any nominated gene to the pathology of associated disease. In this study, we have experimentally shown multiple cellular/physiological results that raise the possibility that TMEM175 is at least in part responsible for the increased risk of PD from the third-most significant PD GWAS peak. Cyclin-G–associated kinase (GAK) is a candidate for this GWAS peak because of its interaction with LRRK2 (1, 40). Lysosomal pH was altered and catalytic capacity of the lysosome was decreased by the depletion of TMEM175, as illustrated by the decreased activity of major lysosomal proteases. In TMEM175-defecient cells, autophagosome clearance was thus delayed with accumulation of autophagic substrates. Mitochondrial energetic capacity was also reduced potentially through impairment in maintaining a functional mitochondrial pool and providing sufficient metabolite to fuel oxidative phosphorylation. Taking these data together, we find that deficiency of TMEM175 leads to increased formation of phosphorylated α-synuclein aggregates, potentially contributed by impaired lysosomal and mitochondrial function. We suggest that TMEM175, like GAK, should be considered a candidate based on functional data. These data demonstrate links to two established PD genetic risk factors: α-synuclein, through increased α-synuclein aggregation; and GBA, through reduced GBA activity in TMEM175-deficient cells. It was noted in the most recent meta-analysis that two independent signals are present in the Chr 4:951,947 GWAS peak (1), raising the possibility that variants in both GAK and TMEM175 could be contributing to disease risk. Similarly, genes in this genomic region may be involved in the same functional pathways.

Dysregulation of ion currents across lysosomal membrane and lysosomal pH alters lysosomal function, and disruption of channel function has been implicated in neurological diseases, including PD. In familial PD, disruption of ATP13A2, which regulates cation transport across lysosomes, leads to dysfunctional lysosomal degradation of proteins and autophagosomes via impaired lysosomal acidification (8, 9). Overexpression of two-pore channels, which mediate endolysosomal Ca^{2+} signals, alkalinizes lysosomal

Downloaded at Palestinian Territory, occupied on December 16, 2021
www.manaraa.com

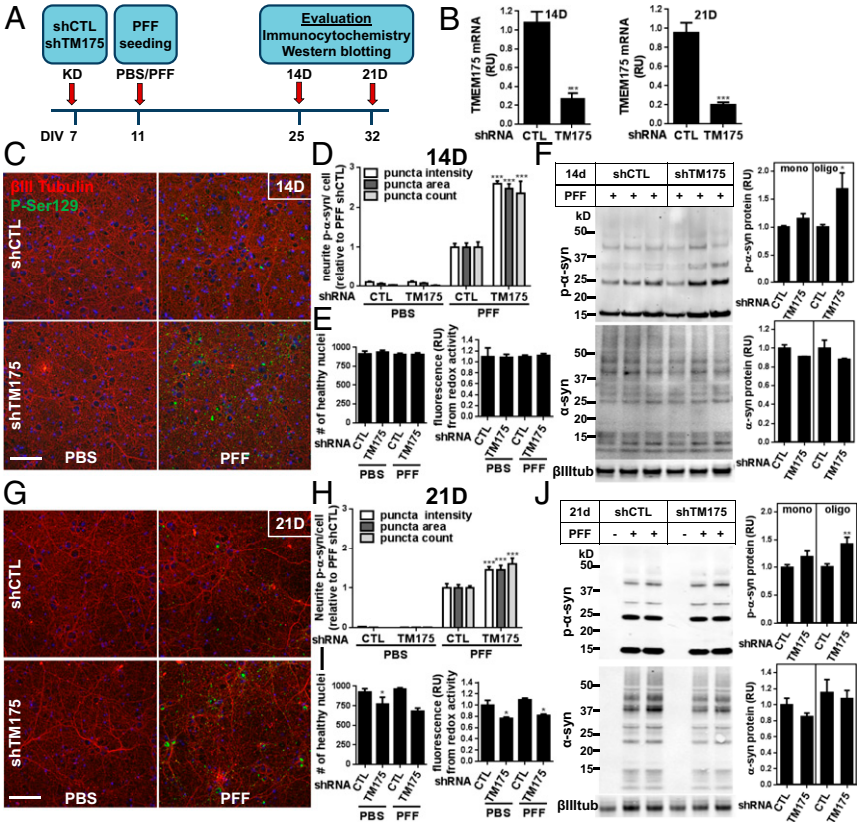

Fig. 4. TMEM175 deficiency increases phosphorylated α-synuclein aggregates in rat primary hippocampal neurons. (*A*) Diagram depicting the experimental design of PFF-seeding model. (*B*) Levels of TMEM175 mRNA from rat hippocampal cells treated with control shRNA (shCTL) or TMEM175 targeting shRNA (shTM175) at 14 and 21 d after PFF. (*C* and *G*) Immunocytochemistry staining of phosphorylated α-synuclein (p-a-syn) aggregate (green) and βIII-tubulin outlining neuronal cell body and neurites (red) at 14 d (*C*,14 d) and 21 d (*G*, 21 d) after PBS/PFF treatment in control (shCTL) and TMEM175 (shTM175) targeting shRNA infected neurons. Blue indicates nuclear staining by Hoechst. (Scale bars, 100 μm.) (*D* and *H*) Quantification of intensity, area and number of aggregates was plotted ($n = 3$). (*E* and *I*) Cell viability was assessed by the number of healthy nuclei (*Left*) and metabolic activity (*Right*) ($n = 3$). (*F* and *J*) Protein amounts of phosphorylated α-synuclein (*Upper*) and total α-synuclein (*Lower*) aggregate in insoluble fraction were quantified by Western blotting, and intensity of monomer and oligomers normalized to tubulin was plotted on the right ($n = 3$–5). Data presented are mean + SEM. Student *t* test in *B*; two-way ANOVA in *D* and *H*; Bonferroni's test in *E*, *F*, *I*, and *J* $*P < 0.05$, $**P < 0.01$, and $***P < 0.001$. shCTL vs. shTM175.

pH to specifically inhibit autophagosomal-lysosomal fusion (41) and are also shown to act downstream of pathogenic leucine-rich repeat kinase 2 (LRRK2) to regulate trafficking within the endo-lysosomal system (42). This evidence stresses the importance of ion current regulation in lysosomal function in PD, and the association of TMEM175 with sporadic PD would further support this pathway as a potential area of intervention for disease-modification therapies. Depletion of TMEM175 leads to unstable pH and the impairment of lysosomal function via decreased protease and GBA activity, the enzymatic function of which is also influenced by the pH of the surrounding environment. Whether the integrity of the lysosome is also compromised by the dysregulation of lysosomal pH requires further investigation; however, complete abrogation of TMEM175 resulted in decreased protein levels of mature CTSD, CTSB, and LAMP1, suggesting that the absence of TMEM175 contributes to early disintegration of dysfunctional lysosomes.

It is important to notice that this impairment of lysosomal catalytic activity also resulted in decreased capacity of macroautophagy, where enzymatic degradation after fusion of the autophagosome to lysosome is critical for complete turnover of unwanted proteins and organelles. Inhibition of basal autophagy is particularly detrimental in neurons that are postmitotic and cannot dilute unfolded proteins or damaged organelles through cell division (43, 44). TMEM175 depletion led to accumulation of autophagy substrates and accelerated fusion of autophagosomes to lysosomes. Given that the formation of autophagosomes is mildly affected by TMEM175 deficiency, these results suggest that decreased lysosomal catalytic activity by TMEM175 deficiency also impairs lysosomal capacity to clear autophagosomes, and thus stalls the completion of autophagy. Cellular fusion of autophagosomes to lysosomes might be increased, in part, as an adaptive response to compensate for stalled degradation of autophagosomes.

The impact of mitigated lysosomal function culminates when cells are challenged with a proteostatic burden, such as α-synuclein aggregates, which are handled by various mechanisms that converge on lysosomal degradation (45). Depletion of TMEM175 resulted in increased aggregate formation in the α-synuclein PFF seeding model, where endocytosed PFF seeds induce endogenous α-synuclein recruitment and aggregation (39). Importantly, there was no difference in the uptake of α-synuclein PFF seeds between control and TMEM175-depleted cells (Fig. S4*D*), suggesting the effect of impaired lysosomal degradation by TMEM175 depletion manifested during the maturation of phosphorylated, insoluble α-synuclein aggregates. Similarly, impaired lysosomes in TMEM175-deficient cells may simply be unable to handle α-synuclein aggregates, which are also resistant to autophagic degradation, reenforcing the vicious cycle of aggregate maturation and inhibition of macroautophagy. However, exactly which parts of any cellular attempt to resolve α-synuclein aggregation are compromised by lysosomal dysfunction resulting from the depletion TMEM175 remains to be studied. The PFF seeding model we adopted was designed to induce minimal cellular toxicity. Hence, we could not determine if TMEM175 KD leads to synergistically increased susceptibility to PFF-induced cell death. Rather, we focused on initial processing/aggregation events of α-synuclein aggregates that we believe to be far upstream from actual cell death, and more proximal to the early cellular insults/stress in the disease. As cellular models of α-synuclein aggregate-mediated cell death become better understood, a logical next step in this research would be to investigate whether TMEM175 deficiency renders cells more vulnerable to aggregate-induced cell death.

It is also important that impaired autophagy might link TMEM175 deficiency to decrease in mitochondrial energetic capacity. Direct inhibition of autophagy through genetic and pharmacological methods was shown to decrease mitochondrial oxygen consumption and energy production, through accumulation of dysfunctional mitochondria and reduced availability of

Downloaded at Palestinian Territory, occupied on December 16, 2021
www.manaraa.com

metabolites to fuel oxidative phosphorylation (34, 35, 46, 47). Decreased mitochondrial respiration and ATP generation in TMEM175-deficient cells could also be caused by these mechanisms. Although the exact mechanism remains to be elucidated, mitochondrial dysfunction could independently increase the risk of PD by promoting the loss of dopaminergic neurons through production of oxidative stress, energy depletion, and ultimately cell death (48, 49).

Together, these findings establish TMEM175 as a potential risk factor and candidate point of intervention for PD with both genetic and biological evidence tying TMEM175, lysosomal function, macroautophagy, and mitochondrial function to α-synucleinopathy.

Methods

Isolation of Lysosomal Fraction. Lysosomal fraction was isolated by differential sedimentation in in sucrose homogenization buffer (0.25 M sucrose, 20 mM Hepes). Details are provided in *SI Methods*.

Lysosomal Enzyme Activity Assay. CTSD and CTSB activity was measured using a cathepsin D and B activity assay kit (Abcam, Ab65302, Ab65300), according to the manufacturer's instructions. Details are provided in *SI Methods*.

Lysosome pH Imaging and Lysosomal Staining. Lysosome pH measurement was adapted from a previously described method (29). Details are provided in *SI Methods*.

Mitochondrial Analysis. Mitochondrial oxygen consumption was measured according to the instruction of XF Cell Mito Stress Test Kit (Seahorse Bioscience). Details are provided in *SI Methods*.

α-Synuclein PFF Seeding. PFF was prepared according to previously described method (50) using human α-synuclein (rPeptide, S-1001-2). Details are provided in *SI Methods*.

Immunocytochemistry. Cells were fixed with 4% (vol/vol) paraformaldehyde/4% (wt/vol) sucrose. After primary and secondary antibody staining and rinsing, antibody-specific fluorescence was visualized with imaging using ArrayScan XTI Live High Content Platform (Thermo Fisher). Details are provided in *SI Methods*. See Table S1 for a list of antibodies used.

Statistical Analyses. Statistical analysis was done by the GraphPad Prism v7.0 (GraphPad Software). Details are provided in *SI Methods*.

ACKNOWLEDGMENTS. The authors thank Jun Zhuang and Katie DiFelice for TMEM175 siRNA-cholesterol conjugates used for rat neuron work; and Dr. Robert Plenge for his support of the work.

1. Nalls MA, et al. (2014) Large-scale meta-analysis of genome-wide association data identifies six new risk loci for Parkinson's disease. *Nat Genet* 56(9):1–7.
2. Gusev A, et al. (2016) Integrative approaches for large-scale transcriptome-wide association studies. *Nat Genet* 48(3):245–252.
3. Zhu Z, et al. (2016) Integration of summary data from GWAS and eQTL studies predicts complex trait gene targets. *Nat Genet* 48(5):481–487.
4. Clark LN, et al. (2007) Mutations in the glucocerebrosidase gene are associated with early-onset Parkinson disease. *Neurology* 69(12):1270–1277.
5. Neumann J, et al. (2009) Glucocerebrosidase mutations in clinical and pathologically proven Parkinson's disease. *Brain* 132(Pt 7):1783–1794.
6. Mazzulli JR, et al. (2011) Gaucher disease glucocerebrosidase and α-synuclein form a bidirectional pathogenic loop in synucleinopathies. *Cell* 146(1):37–52.
7. Ramirez A, et al. (2006) Hereditary parkinsonism with dementia is caused by mutations in ATP13A2, encoding a lysosomal type 5 P-type ATPase. *Nat Genet* 38(10):1184–1191.
8. Usenovic M, Tresse E, Mazzulli JR, Taylor JP, Krainc D (2012) Deficiency of ATP13A2 leads to lysosomal dysfunction, α-synuclein accumulation, and neurotoxicity. *J Neurosci* 32(12):4240–4246.
9. Dehay B, et al. (2012) Loss of P-type ATPase ATP13A2/PARK9 function induces general lysosomal deficiency and leads to Parkinson disease neurodegeneration. *Proc Natl Acad Sci USA* 109(24):9611–9616.
10. Zimprich A, et al. (2011) A mutation in VPS35, encoding a subunit of the retromer complex, causes late-onset Parkinson disease. *Am J Hum Genet* 89(1):168–175.
11. Miura E, et al. (2014) VPS35 dysfunction impairs lysosomal degradation of α-synuclein and exacerbates neurotoxicity in a *Drosophila* model of Parkinson's disease. *Neurobiol Dis* 71:1–13.
12. Tang FL, et al. (2015) VPS35 deficiency or mutation causes dopaminergic neuronal loss by impairing mitochondrial fusion and function. *Cell Reports* 12(10):1631–1643.
13. Tsika E, et al. (2014) Parkinson's disease-linked mutations in VPS35 induce dopaminergic neurodegeneration. *Hum Mol Genet* 23(17):4621–4638.
14. Youle RJ, Narendra DP (2011) Mechanisms of mitophagy. *Nat Rev Mol Cell Biol* 12(1):9–14.
15. Kane LA, et al. (2014) PINK1 phosphorylates ubiquitin to activate Parkin E3 ubiquitin ligase activity. *J Cell Biol* 205(2):143–153.
16. Kazlauskaite A, et al. (2014) Parkin is activated by PINK1-dependent phosphorylation of ubiquitin at Ser65. *Biochem J* 460(1):127–139.
17. Lazarou M, et al. (2015) The ubiquitin kinase PINK1 recruits autophagy receptors to induce mitophagy. *Nature* 524(7565):309–314.
18. Koyano F, et al. (2014) Ubiquitin is phosphorylated by PINK1 to activate parkin. *Nature* 510(7503):162–166.
19. Kitada T, et al. (1998) Mutations in the parkin gene cause autosomal recessive juvenile parkinsonism. *Nature* 392(6676):605–608.
20. Valente EM, et al. (2004) Hereditary early-onset Parkinson's disease caused by mutations in PINK1. *Science* 304(5674):1158–1160.
21. Di Fonzo A, et al. (2009) FBXO7 mutations cause autosomal recessive, early-onset parkinsonian-pyramidal syndrome. *Neurology* 72(3):240–245.
22. Paisán-Ruiz C, et al. (2010) Early-onset L-dopa-responsive parkinsonism with pyramidal signs due to ATP13A2, PLA2G6, FBXO7 and Spatacsin mutations. *Mov Disord* 25(12):1791–1800.
23. Burchell VS, et al. (2013) The Parkinson's disease-linked proteins Fbxo7 and Parkin interact to mediate mitophagy. *Nat Neurosci* 16(9):1257–1265.
24. Burman JL, Yu S, Poole AC, Decal RB, Pallanck L (2012) Analysis of neural subtypes reveals selective mitochondrial dysfunction in dopaminergic neurons from parkin mutants. *Proc Natl Acad Sci USA* 109(26):10438–10443.
25. Matsui H, et al. (2013) PINK1 and parkin complementarily protect dopaminergic neurons in vertebrates. *Hum Mol Genet* 22(12):2423–2434.
26. Petrucelli L, et al. (2002) Parkin protects against the toxicity associated with mutant alpha-synuclein: Proteasome dysfunction selectively affects catecholaminergic neurons. *Neuron* 36(6):1007–1019.
27. Todd AM, Staveley BE (2008) Pink1 suppresses alpha-synuclein-induced phenotypes in a *Drosophila* model of Parkinson's disease. *Genome* 51(12):1040–1046.
28. Chapel A, et al. (2013) An extended proteome map of the lysosomal membrane reveals novel potential transporters. *Mol Cell Proteomics* 12(6):1572–1588.
29. Cang C, Aranda K, Seo YJ, Gasnier B, Ren D (2015) TMEM175 is an organelle K(+) channel regulating lysosomal function. *Cell* 162(5):1101–1112.
30. Kiffin R, et al. (2007) Altered dynamics of the lysosomal receptor for chaperone-mediated autophagy with age. *J Cell Sci* 120(Pt 5):782–791.
31. Kundra R, Kornfeld S (1999) Asparagine-linked oligosaccharides protect Lamp-1 and Lamp-2 from intracellular proteolysis. *J Biol Chem* 274(43):31039–31046.
32. Xu H, Ren D (2015) Lysosomal physiology. *Annu Rev Physiol* 77(1):57–80.
33. Mijaljica D, Prescott M, Devenish RJ (2007) Different fates of mitochondria: Alternative ways for degradation? *Autophagy* 3(1):4–9.
34. Guo JY, et al. (2011) Activated Ras requires autophagy to maintain oxidative metabolism and tumorigenesis. *Genes Dev* 25(5):460–470.
35. Yang S, et al. (2011) Pancreatic cancers require autophagy for tumor growth. *Genes Dev* 25(7):717–729.
36. Fukasawa Y, et al. (2015) MitoFates: Improved prediction of mitochondrial targeting sequences and their cleavage sites. *Mol Cell Proteomics* 14(4):1113–1126.
37. Calvo SE, Clauser KR, Mootha VK (2016) MitoCarta2.0: An updated inventory of mammalian mitochondrial proteins. *Nucleic Acids Res* 44(D1):D1251–D1257.
38. Volpicelli-Daley LA, et al. (2016) G2019S-LRRK2 expression augments α-synuclein sequestration into inclusions in neurons. *J Neurosci* 36(28):7415–7427.
39. Volpicelli-Daley LA, et al. (2011) Exogenous α-synuclein fibrils induce Lewy body pathology leading to synaptic dysfunction and neuron death. *Neuron* 72(1):57–71.
40. Beilina A, et al.; International Parkinson's Disease Genomics Consortium; North American Brain Expression Consortium (2014) Unbiased screen for interactors of leucine-rich repeat kinase 2 supports a common pathway for sporadic and familial Parkinson disease. *Proc Natl Acad Sci USA* 111(7):2626–2631.
41. Lu Y, et al. (2013) Two pore channel 2 (TPC2) inhibits autophagosomal-lysosomal fusion by alkalinizing lysosomal pH. *J Biol Chem* 288(33):24247–24263.
42. Hockey LN, et al. (2015) Dysregulation of lysosomal morphology by pathogenic LRRK2 is corrected by TPC2 inhibition. *J Cell Sci* 128(2):232–238.
43. Hara T, et al. (2006) Suppression of basal autophagy in neural cells causes neurodegenerative disease in mice. *Nature* 441(7095):885–889.
44. Komatsu M, et al. (2007) Essential role for autophagy protein Atg7 in the maintenance of axonal homeostasis and the prevention of axonal degeneration. *Proc Natl Acad Sci USA* 104(36):14489–14494.
45. Xilouri M, Brekk OR, Stefanis L (2013) α-Synuclein and protein degradation systems: a reciprocal relationship. *Mol Neurobiol* 47(2):537–551.
46. Borkowska J, Schwartz RA, Kotulska K, Jozwiak S (2011) Tuberous sclerosis complex: Tumors and tumorigenesis. *Int J Dermatol* 50(1):13–20.
47. Liang X, et al. (2012) Inhibiting systemic autophagy during interleukin 2 immunotherapy promotes long-term tumor regression. *Cancer Res* 72(11):2791–2801.
48. Exner N, Lutz AK, Haass C, Winklhofer KF (2012) Mitochondrial dysfunction in Parkinson's disease: Molecular mechanisms and pathophysiological consequences. *EMBO J* 31(14):3038–3062.
49. Vila M, Ramonet D, Perier C (2008) Mitochondrial alterations in Parkinson's disease: New clues. *J Neurochem* 107(2):317–328.
50. Volpicelli-Daley LA, Luk KC, Lee VM-Y (2014) Addition of exogenous α-synuclein preformed fibrils to primary neuronal cultures to seed recruitment of endogenous α-synuclein to Lewy body and Lewy neurite-like aggregates. *Nat Protoc* 9(9):2135–2146.
51. Ma L, et al. (2010) Genome-wide microarray analysis of the differential neuroprotective effects of antioxidants in neuroblastoma cells overexpressing the familial Parkinson's disease alpha-synuclein A53T mutation. *Neurochem Res* 35(1):130–142.

Downloaded at Palestinian Territory, occupied on December 16, 2021
www.manaraa.com